Desalination and Water Treatment
www.deswater.com

doi:10.5004/dwt.2021.27128

224 (2021) 178–186
June

Desorption and recovery of fluoride adsorbed by the aluminum-loaded chelating resin

Ke Jiang*, Xiangnong Zeng

Changsha Environmental Protection College, Changsha 410004, China, Tel. +86 13874913813; Fax: +86 0731 85622912; emails: j_k8663661@126.com (K. Jiang), 369752187@qq.com (X. Zeng)

Received 25 August 2020; Accepted 12 February 2021

ABSTRACT

The desorption ability of metal-loaded resins is the key factor limiting the application for fluoride removal. In this study, the desorption behaviors of fluoride adsorbed by an aluminum-loaded chelating resin (D751) were investigated at relatively low liquid/solid ratios. The feasibility of recovering fluoride from the desorption solution was determined by the experiments and the thermodynamic modeling. The results showed that NaOH was a more suitable desorption reagent than HCl. The desorption ratio of fluoride surpassed 80% after 30 min in 2.0 mol/L NaOH. The fluoride concentration of the desorption solution was 2.8–12.8 g/L with a F/Al molar ratio of 1.0. The F/Al molar ratio and reaction pH were the main factors determining the recovery of fluoride from the desorption solution. More than 80% of the fluoride was recovered from the desorption solution as cryolite products after the addition of HF and HCl. The residual fluoride concentration decreased from 3,508.2 mg/L to 401.8–482.5 mg/L at a F/Al molar ratio of 5.0–6.0 and at pH 6.0.

Keywords: Fluoride; Aluminum-loaded resin; Ion exchange; Desorption; Cryolite

1. Introduction

Fluoride is a major contaminant worldwide as fluoride-containing wastewaters are produced by the semiconductor, fluorine chemical, aluminum electrolysis, and photovoltaic industries [1–3]. Excess fluoride in wastewater has serious detrimental effects on the environment and human beings [4]. However, fluorite is a precious non-metallic ore that is currently in the midst of a worldwide shortage [5]. Therefore, the efficient removal and recovery of fluoride from wastewater would not only benefit the environment but would also be of great economic value.

Chemical precipitation and coagulation are commonly used treatment methods for wastewater with high fluoride content [6,7]. This approach produces large amounts of non-reusable, low-quality sludge that is expensive to dispose of. To recover qualified calcium fluoride or cryolite products, crystallization reactors are developed and used for chemical precipitation [8,9]. However, crystallization and chemical precipitation are not suitable for the treatment of wastewater with low fluoride content and complicated components. Adsorption and ion exchange have been identified as potentially effective approaches for the removal of low to medium levels of fluoride. The adsorbents used generally include natural macromolecules, inorganic compounds, rare earth elements, and clay materials, etc. [10–14]. These adsorbents are best suited for the thorough removal of trace fluoride via monolayer adsorption [14]. However, the regeneration and desorption efficiency of these adsorbents need to be explored to improve their reusability. Ion exchange resins are considered to be promising materials for fluoride removal, but their fluoride adsorption capacities decrease significantly when SO_4^{2-}, NO_3^-, or Cl^- are present [15].

* Corresponding author.

To improve fluoride adsorption selectivity, metal-loaded chelating resins can be used. Chelating resins, such as the iminodiacetic acid resin or the amino phosphoric acid resin, benefit from the coordination between the metal ions (La^{3+}, Ce^{3+}, Zr^{4+}, Al^{3+}, etc.) and fluoride [16–19]. One possible adsorption mechanism by which Al-loaded iminodiacetic acid resin (TP208) absorbs fluoride can be seen [20] in Eqs. (1) and (2). Fluoride can be adsorbed and removed by the strong coordination among the iminodiacetic acid group, Al^{3+}, and F^-. The metal-loaded chelating resins have been proved effective for fluoride removal with high adsorption selectivity [20–23]:

$$R–CH_2–N–CH_2–COO^- + Al^{3+} = R–CH_2–N–CH_2–COO^–Al^{3+} \quad (1)$$

$$R–CH_2–N–CH_2–COO^–Al^{3+} + xF^- = R–CH_2–N–CH_2–COO^–AlF_x^{3-x} \quad (2)$$

To decrease adsorption costs, the chelating resins should also be desorbed for cyclic utilization. The desorption ability of metal-loaded resins becomes the key factor limiting the application of this method. Studies on the desorption rate of fluoride and on the treatment of the desorption solution are relatively rare. One such study by Paudyal et al. [24,25] successfully used NaOH solution for the desorption of Zr-loaded resin. However, a large amount of desorption solution is produced at a relatively high liquid/solid ratio (e.g., 400:1). Furthermore, the treatment and recovery of fluoride from desorption solutions have not been addressed. If the desorption solution can not be treated properly, new fluoride pollution will be produced, and fluoride resources in the desorption solution will be wasted.

Our previous research has shown that metal ions are desorbed from the chelating resin alongside fluoride into the solution [26]. Considering the value of metal ions (La^{3+}, Ce^{3+}, and Zr^{4+}) and their inevitable loss during desorption experiments, the cheaper Al^{3+} ion was chosen for loading the iminodiacetic acid chelating resin (D751). After desorption, aluminum and fluoride were shown to be the main components in the desorption solution, and from this solution cryolite (Na_3AlF_6) was identified as the preferred recovery product [9,27]. This study assessed the feasibility of desorption and recovery of fluoride from the Al-loaded D751 resin. The desorption behaviors of fluoride on the resin were investigated with low liquid/solid ratios using static desorption experiments. The optimal conditions for the recovery of cryolite from the desorption solution were determined using thermodynamic modeling and batch experiments.

2. Materials and methods

2.1. Materials

D751 resin, an iminodiacetic acid chelating resin in a sodium salt form, was donated by Wandong Resin Technology Co., Ltd., of China. Before loading with aluminum ions, the original D751 resin was pretreated with 10% hydrochloric acid, 10% sodium hydroxide, and deionized water successively until a neutral pH was achieved. All reagents, including NaF, NaOH, HCl, HF, and $Al_2(SO_4)_3$ were analytical grade.

2.2. Resin loading and fluoride adsorption

The D751 resin was loaded with Al^{3+} ions by submerging it in a 0.5 mol/L of $Al_2(SO_4)_3$ solution for 2 h. Then the aluminum-loaded resin was washed with distilled water to regain a neutral pH, and dried at 60°C for 24 h.

The loaded D751 resin (50.0 g) was mixed together with 4.0 L of NaF solution containing 1,000 mg/L fluorides and stirred for 2 h at 25°C for adsorption. After adsorption, the residual fluoride concentration of the suspension was measured. The resin with adsorbed fluoride was washed with 100 mL distilled water and dried at 60°C for 24 h.

2.3. Desorption experiments

The adsorbed D751 resin (5.0 g) was mixed with 10–50 mL of desorption reagents (NaOH or HCl) and stirred for 5–90 min at 25°C. After stirring, the residual concentrations of fluoride and aluminum in the desorption solution were measured.

2.4. Recovery of the desorption solution

At the end of the desorption experiment, the solution had a fluoride concentration of 3,508.2 mg/L and an aluminum concentration of 5,041.8 mg/L. Hydrochloric acid (HCl, 5 mol/L) and hydrofluoric acid (HF, 40% w/v) were then added into this desorption solution (250 mL) and it was stirred for 60 min at 25°C. Then the residual concentration of fluoride in the treated desorption solution was measured. The precipitate was filtered, washed with 100 mL distilled water, and dried at 60°C for 24 h.

2.5. Analysis

The reaction pH was measured using a pH meter, and the fluoride concentration was measured using an ion-selective electrode. The aluminum concentration was analyzed by inductively coupled plasma atomic emission spectroscopy (ICAP-7200). The resin was analyzed using infrared spectroscopy (Nicolet IS50, USA) and an energy dispersive spectrometer (JSM-7900F, Japan). The precipitate was analyzed by X-ray diffraction (XRD; Bruker D8 Advance, Germany).

The adsorption capacity of the resin (Q_a) was determined using Eq. (3):

$$Q_a = \frac{(c_0 - c_i) \times V_{NaF}}{m_R} \quad (3)$$

where c_0 and c_i were the initial and residual fluoride concentrations, respectively, of the NaF solution; V_{NaF} was the volume of NaF solution; and m_R was the mass of the loaded resin.

The desorption ratio of fluoride (D_F) was determined using Eq. (4):

$$D_F = \frac{c_d \times V_d}{(Q_a \times m_a)} \times 100\% \quad (4)$$

where c_d was the fluoride concentration of desorption solution; V_d was the volume of desorption solution; and m_a was the mass of the adsorbed resin.

The recovery ratio of fluoride (R_F) was determined using Eq. (5):

$$R_F = \frac{\left(c_d \times V_d - V_R \times c_R\right)}{\left(c_d \times V_d\right)} \times 100\% \quad (5)$$

where c_R was the residual fluoride concentration of treated desorption solution; and V_R was the residual volume of treated desorption solution.

The comprehensive recovery ratio of fluoride ($R_{F,C}$) was determined using Eq. (6):

$$R_{F,C} = \frac{\left(c_d \times V_d + c_{\mathrm{HF}} \times V_{\mathrm{HF}} - V_R \times c_R\right)}{\left(c_d \times V_d\right)} \times 100\% \quad (6)$$

where c_{HF} was the fluoride concentration of hydrofluoric acid; and V_{HF} was the volume of the hydrofluoric acid.

2.6. Thermodynamic modeling

The possible species in the Al^{3+}–Na^+–F^-–H^+–H_2O system mainly included Al^{3+}, Na^+, F^-, H^+, AlF^{2+}, AlF_2^+, AlF_3(aq), AlF_4^-, AlF_5^{2-}, AlF_6^{3-}, $Al(OH)^{2+}$, $Al(OH)_2^+$, $Al(OH)_3$(aq), $Al(OH)_4^-$, HF, HF_2^-, Na_3AlF_6(s), $NaAlF_4$(s), and $Al(OH)_3$(s). The ion and solid-phase equilibria are listed in Table 1. Eqs. (7)–(21) correlate the thermodynamic equilibrium constants of the different complexes to their molar concentrations.

The total concentrations of aluminum, sodium, and fluoride, denoted as $C_{T,\mathrm{Al}}$, $C_{T,\mathrm{Na}}$, and $C_{T,\mathrm{F}}$, were calculated as the sums of the concentrations of their complexes and free ions as illustrated in Eqs. (22)–(24):

$$\begin{aligned} C_{T,\mathrm{Al}} = {} & c(\mathrm{Al^{3+}}) + c(\mathrm{AlF^{2+}}) + c(\mathrm{AlF_2^+}) + c(\mathrm{AlF_3})_{\mathrm{aq}} + \\ & c(\mathrm{AlF_4^-}) + c(\mathrm{AlF_5^{2-}}) + c(\mathrm{AlF_6^{3-}}) + c[\mathrm{Al(OH)^{2+}}] + \\ & c[\mathrm{Al(OH)_2^+}] + c[\mathrm{Al(OH)_3}]_{\mathrm{aq}} + c[\mathrm{Al(OH)_4^-}] \end{aligned} \quad (22)$$

$$C_{T,\mathrm{Na}} = c(\mathrm{Na^+}) \quad (23)$$

$$\begin{aligned} C_{T,\mathrm{F}} = {} & c(\mathrm{F^-}) + c(\mathrm{HF}) + c(\mathrm{HF_2^-}) + c(\mathrm{AlF^{2+}}) + 2c(\mathrm{AlF_2^+}) + \\ & 3c(\mathrm{AlF_3})_{\mathrm{aq}} + 4c(\mathrm{AlF_4^-}) + 5c(\mathrm{AlF_5^{2-}}) + 6c(\mathrm{AlF_6^{3-}}) \end{aligned} \quad (24)$$

The independence components in the system were $c(Al^{3+})$, $c(Na^+)$, $c(F^-)$, and $c(H^+)$. According to Eqs. (7)–(24), if the $C_{T,\mathrm{F}}/C_{T,\mathrm{Al}}$, and $C_{T,\mathrm{Na}}$ values were given; the predominance diagrams of $\log C_{T,\mathrm{F}}$ vs. pH could be determined. If the $C_{T,\mathrm{Na}}$ and pH values were given, the predominance diagrams of $\log C_{T,\mathrm{F}}$ vs. $C_{T,\mathrm{F}}/C_{T,\mathrm{Al}}$ could be determined.

According to Eqs. (10)–(24), if the $C_{T,\mathrm{F}}$, $C_{T,\mathrm{Al}}$, and pH values were given; the distribution ratio of the fluoride species ($\alpha_{\mathrm{F},i}$) and aluminum species ($\alpha_{\mathrm{Al},i}$) was determined using Eqs. (25) and (26), respectively.

$$\alpha_{\mathrm{F},i} = \frac{100\% \times c_{\mathrm{F},i}}{C_{T,\mathrm{F}}} \quad (25)$$

$$\alpha_{\mathrm{Al},i} = \frac{100\% \times c_{\mathrm{Al},i}}{C_{T,\mathrm{Al}}} \quad (26)$$

where $c_{\mathrm{F},i}$ and $c_{\mathrm{Al},i}$ were the concentration of the fluoride and aluminum species, respectively.

3. Results and discussion

3.1. Characteristic of the resin

Fig. 1 shows the IR Spectra of the resin. Fig. 2 shows the EDS analysis of the fluoride-absorbed resin.

According to Eq. (3), the adsorption capacity of the resin was 35.1 mg/g. The aluminum and iminodiacetic acid on the resin were both essential for the adsorption of fluoride. As shown in Fig. 1, in the original resin the O–H stretching vibration peak was apparent at 3,390.13 cm^{-1} but was significantly reduced after loading the resin with aluminum. This indicated that the OH^- within the resin was neutralized during the pretreatment process. The C=O stretching vibration was observed at 1,614.82 cm^{-1} in the original resin but shifted to 1,651.99 cm^{-1} in the aluminum-loaded resin. The C–O stretching vibration was present at 1,488.47 cm^{-1} in the original resin but moved to 1,397.79 cm^{-1} in the aluminum-loaded resin. Therefore, the –COOH of the resin appeared to interact with aluminum, based on the changes to C=O and C–O after aluminum loading. In addition, the C=O stretching vibration only slightly decreased after fluoride adsorption, and the C–F stretching vibration could be observed at 1,127.29 cm^{-1}. The fluoride might be removed as a function of both Al–F and C–F by electrostatic adsorption, Lewis acid–base interaction, and complexation [20,22]. According to the EDS analysis, the average mass ratios of F, Na, and Al were 41.82%, 37.73%, and 20.45%, respectively. This demonstrated that fluoride was effectively absorbed onto the aluminum-loaded resin. In addition, some fine particles were observed in the SEM images, which might be Na, Al, and F precipitates, such as Na_3AlF_6, during the adsorption process.

3.2. Desorption behavior of the absorbed resin

Fig. 3 shows the influence of reagents on the desorption ratio of fluoride. The desorption of fluoride reached equilibrium within 30 min. The equilibrium desorption ratios of fluoride were 78.9% and 27.9% when using NaOH and HCl as the desorption reagents, respectively. The desorption of fluoride was determined by the stability of the iminodiacetic-aluminum complex [26]. In acid conditions, part of the iminodiacetic-aluminum complex was transformed into the iminodiacetic acid, but the iminodiacetic-aluminum complex was still the dominant species. In alkaline conditions, the bond within the iminodiacetic-aluminum complex was broken completely, and aluminum entered the solution with the form of $Al(OH)_4^-$. Therefore, alkaline conditions appeared to favor the desorption of fluoride from the resin.

Fig. 4 shows the influence of reagents concentration on the desorption ratio of fluoride. The desorption ratio of fluoride first increased with NaOH concentration before becoming stable. Approximately 80% of the fluoride was desorbed from the resin with NaOH concentrations of 2.0–10.0 mol/L. The equilibrium between the remaining absorbed fluoride in the resin and the fluoride in the desorption solution occurred at the NaOH concentration of 2 mol/L.

Table 1
Ion and solid-phase equilibria for Al^{3+}–Na^{+}–F^{-}–H^{+}–H_2O system (25°C)

No.	Equilibrium reactions	Equations	Ref.
(7)	$Na_3AlF_6(s) \rightleftharpoons 3Na^+ + Al^{3+} + 6F^-$	$[c(Na^+)]^3 \times c(Al^{3+}) \times [c(F^-)]^6 = 1.46 \times 10^{-34}$	[28]
(8)	$NaAlF_4(s) \rightleftharpoons Na^+ + AlF_4^-$	$c(Na^+) \times c(AlF_4^-) = 10^{-4.92}$	[29]
(9)	$Al(OH)_3(s) \rightleftharpoons Al^{3+} + 3OH^-$	$c(Al^{3+}) \times [c(OH^-)]^3 = 10^{-32.3}$	[30]
(10)	$AlF^{2+} \rightleftharpoons Al^{3+} + F^-$	$\frac{c\left(Al^{3+}\right)\times c\left(F^-\right)}{c\left(AlF^{2+}\right)} = 10^{-7.0}$	[31]
(11)	$AlF_2^+ \rightleftharpoons Al^{3+} + 2F^-$	$\frac{c\left(Al^{3+}\right)\times \left[c\left(F^-\right)\right]^2}{c\left(AlF_2^+\right)} = 10^{-12.7}$	[31]
(12)	$(AlF_3)_{aq} \rightleftharpoons Al^{3+} + 3F^-$	$\frac{c\left(Al^{3+}\right)\times \left[c\left(F^-\right)\right]^3}{c\left(AlF_3\right)_{aq}} = 10^{-16.8}$	[31]
(13)	$AlF_4^- \rightleftharpoons Al^{3+} + 4F^-$	$\frac{c\left(Al^{3+}\right)\times \left[c\left(F^-\right)\right]^4}{c\left(AlF_4^-\right)} = 10^{-19.4}$	[31]
(14)	$AlF_5^{2-} \rightleftharpoons Al^{3+} + 5F^-$	$\frac{c\left(Al^{3+}\right)\times \left[c\left(F^-\right)\right]^5}{c\left(AlF_5^{3-}\right)} = 10^{-20.6}$	[31]
(15)	$AlF_6^{3-} \rightleftharpoons Al^{3+} + 6F^-$	$\frac{c\left(Al^{3+}\right)\times \left[c\left(F^-\right)\right]^6}{c\left(AlF_6^{3-}\right)} = 10^{-20.6}$	[31]
(16)	$Al^{3+} + H_2O \rightleftharpoons Al(OH)^{2+} + H^+$	$\frac{c\left(Al(OH)^{2+}\right)\times c\left(H^+\right)}{c\left(Al^{3+}\right)} = 10^{-4.99}$	[31]
(17)	$Al^{3+} + 2H_2O \rightleftharpoons Al(OH)_2^+ + 2H^+$	$\frac{c\left(Al(OH)_2^+\right)\times \left[c\left(H^+\right)\right]^2}{c\left(Al^{3+}\right)} = 10^{-10.1}$	[31]
(18)	$Al^{3+} + 3H_2O \rightleftharpoons [Al(OH)_3]_{aq} + 3H^+$	$\frac{c\left[Al(OH)_3\right]_{aq}\times \left[c\left(H^+\right)\right]^3}{c\left(Al^{3+}\right)} = 10^{-15.6}$	[31]
(19)	$Al^{3+} + 4H_2O \rightleftharpoons Al(OH)_4^- + 4H^+$	$\frac{c\left[Al(OH)_4\right]^-\times \left[c\left(H^+\right)\right]^4}{c\left(Al^{3+}\right)} = 10^{-23.0}$	[31]
(20)	$HF \rightleftharpoons H^+ + F^-$	$\frac{c\left(F^-\right)\times c\left(H^+\right)}{c\left(HF\right)} = 10^{-3.176}$	[32]
(21)	$HF_2^- \rightleftharpoons H^+ + 2F^-$	$\frac{\left[c\left(F^-\right)\right]^2\times c\left(H^+\right)}{c\left(HF_2^-\right)} = 10^{-3.653}$	[32]

Higher desorption ratios may be achieved by increasing the number of desorption or using ion-exchange columns for continuous desorption.

Fig. 5 shows the desorption ratios of fluoride and its concentrations in the desorption solutions in relation to the volume of the reagents. The liquid/solid ratio of V_d to m_a ranged between 2:1 and 10:1, significantly lower than that (400:1) used in previous studies [24,25]. Both fluoride and aluminum concentrations increased with decreasing desorption reagent volume. The fluoride concentration of the desorption solution was 2.8–12.8 g/L, while the aluminum concentration was 4.0–18.1 g/L. The molar ratio of F/Al in the desorption solution was 0.96–1.00. Their similar molar ratios indicated that aluminum and fluoride were desorbed simultaneously from the resin, which was agreed with our previous adsorption results [26]. The main species of fluoride and aluminum in the desorption solution were F^- and $Al(OH)_4^-$, respectively, according to the distribution ratio of the fluoride species (Figs. S1 and S2).

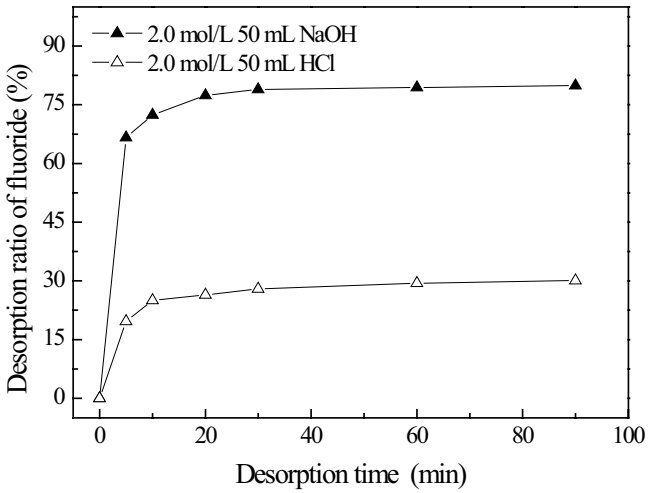

Fig. 3. Influence of reagents on the desorption ratio of fluoride.

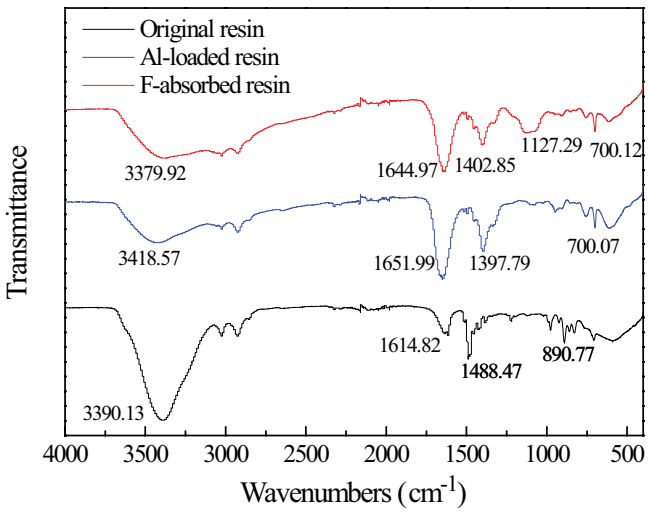

Fig. 1. IR spectra of the loaded resin.

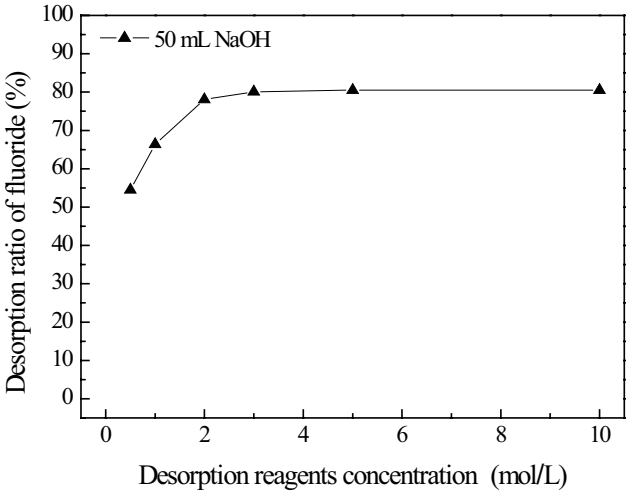

Fig. 4. Influence of reagents concentration on the desorption ratio of fluoride (desorption time = 30 min).

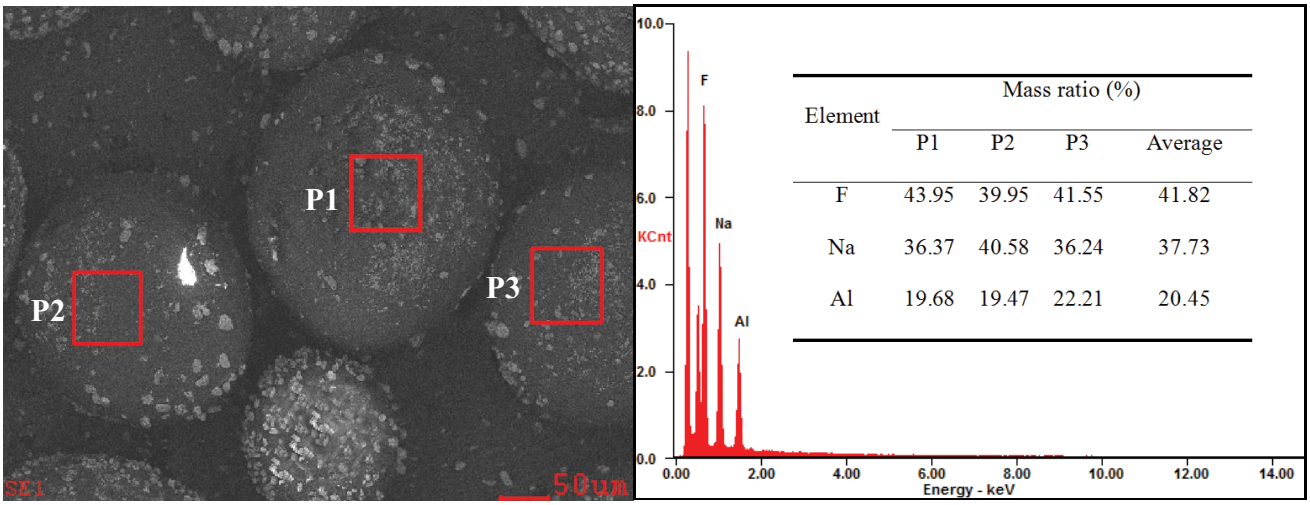

Element	Mass ratio (%)			
	P1	P2	P3	Average
F	43.95	39.95	41.55	41.82
Na	36.37	40.58	36.24	37.73
Al	19.68	19.47	22.21	20.45

Fig. 2. EDS analysis of the fluoride-absorbed resin.

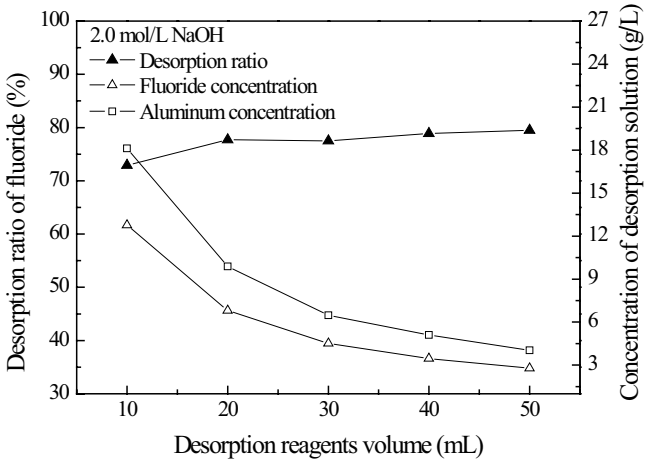

Fig. 5. Influence of reagents volume on desorption (desorption time = 30 min).

Besides, the desorption ratio of fluoride remained between 72.9% and 79.9%. Therefore, the volume of the desorption reagent only slightly influenced the desorption ratio of fluoride. High desorption ratios of fluoride and its highest concentrations in the desorption solution were achieved at relatively low liquid/solid ratios (i.e., 4:1–10:1). The reagent cost was approximately 1%–2.5% of that reported in the literature [24,25]. To better facilitate the goal of recovering fluoride, its concentrations in the desorption solution can be adjusted by decreasing the liquid/solid ratio.

3.3. Predominance diagrams for Al^{3+}–Na^{+}–F^{-}–H^{+}–H_2O system

To guide recovery from the desorption solution, the precipitation–dissolution equilibrium was simulated. Figs. 6 and 7 show the predominance diagrams for Al^{3+}–Na^{+}–F^{-}–H^{+}–H_2O system.

The total equilibrium concentration of sodium ($C_{T,Na}$) was set to 2 mol/L. At an equilibrium F/Al molar ratio of 1.0 in Fig. 6, the predominant solid phases changed from $NaAlF_4$ to $Al(OH)_3$ and Na_3AlF_6 at pH 3.0 and 11.8, respectively. $Al(OH)_3$ was the predominant solid phase from pH 3.0 to pH–11.8. $Al(OH)_3$ and $NaAlF_4$ might precipitate simultaneously from the desorption solution between pH 3.0 and 6.1. $Al(OH)_3$, $NaAlF_4$, and Na_3AlF_6 might precipitate simultaneously at pH > 6.1. At an equilibrium F/Al molar ratio of 6.0, Na_3AlF_6 was precipitated as the predominant solid phase from pH of 0 to 14. Na_3AlF_6 and $NaAlF_4$ might precipitate simultaneously from the desorption solution. The lowest concentration of fluoride occurred at pH 3.5–7.0.

At an equilibrium pH of 6.0 in Fig. 7, the predominant solid phase was $Al(OH)_3$ at a F/Al molar ratio from 1.0 to 3.1. Then Na_3AlF_6 became more stable at F/Al molar ratios above 3.1. Na_3AlF_6 was more easily precipitated than $NaAlF_4$, accompanied by a relatively low concentration of fluoride. In order to obtain a pure Na_3AlF_6 precipitate, the F/Al molar ratio of the desorption solution should be maintained above 3.1 at pH 6.0.

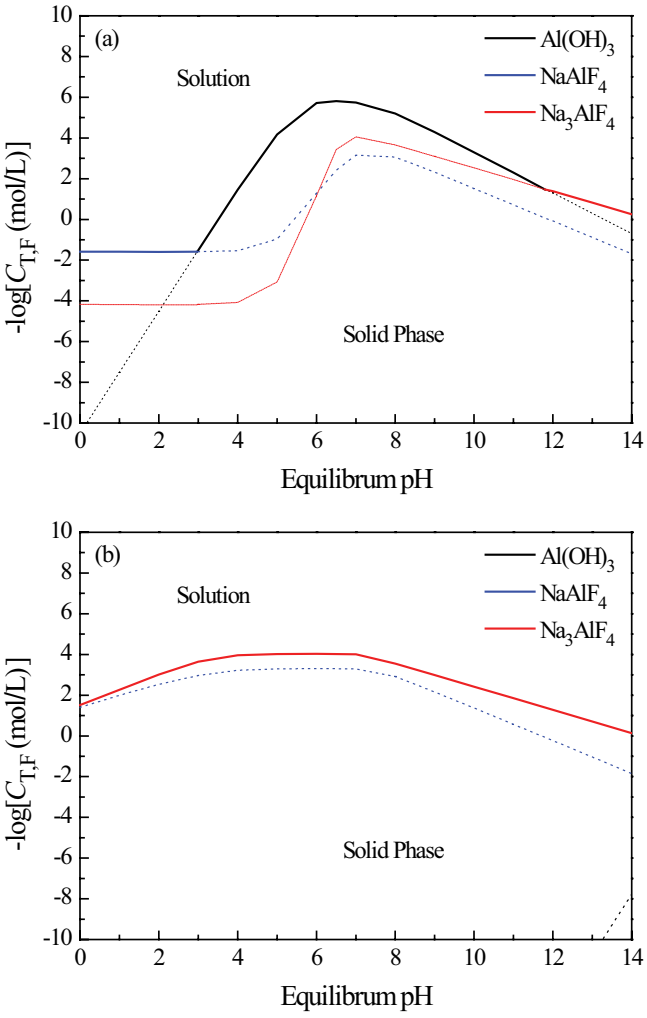

Fig. 6. Predominance diagrams for Al^{3+}–Na^{+}–F^{-}–H^{+}–H_2O system at fixed F/Al ($C_{T,Na}$ = 2 mol/L). Molar ratio of (a) F/Al = 1 and (b) F/Al = 6.

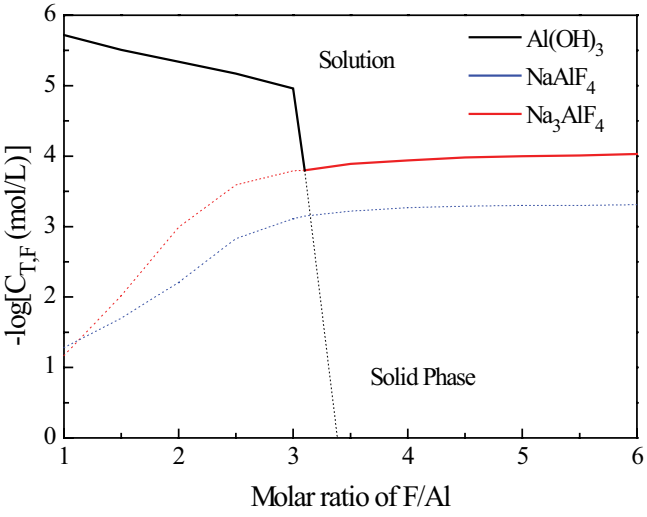

Fig. 7. Predominance diagrams for Al^{3+}–Na^{+}–F^{-}–H^{+}–H_2O system at pH = 6.0 ($C_{T,Na}$ = 2 mol/L).

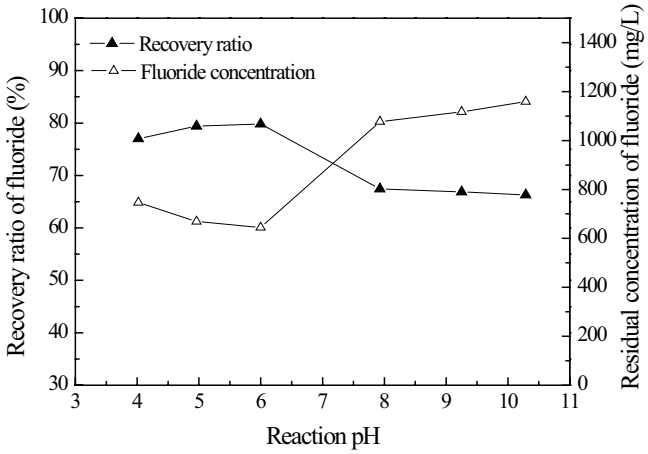

Fig. 8. Influence of reaction pH on the recovery rate of fluoride.

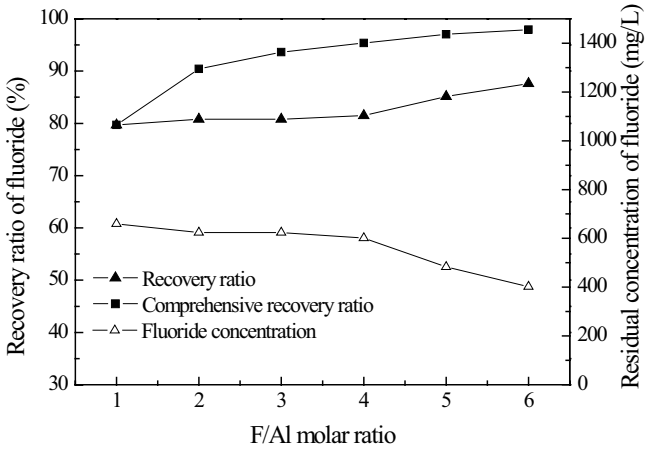

Fig. 9. Influence of F/Al molar ratio on the recovery rate of fluoride (Reaction pH = 6.0 ± 0.1).

3.4. Recovery of the desorption solution

Fig. 8 shows the influence of reaction pH on the recovery rate of fluoride. Fig. 9 shows the influence of the F/Al molar ratio on the recovery rate of fluoride. Fig. 10 shows the XRD spectra of the recovered precipitations.

As shown in Fig. 8, the initial F/Al molar ratio of the desorption solution was 1.0. The residual fluoride concentration of treated desorption solution was 645.1–746.9 mg/L at pH 4.0–6.0, and the recovery ratio of fluoride was 77.0%–79.8%. As shown in Fig. 10a, $NaAlF_4$ made up the majority of the precipitate at pH 6.0. The residual fluoride concentration of treated desorption solution increased to above 1,000 mg/L at pH 7.9–10.3, and the recovery ratio of fluoride decreased to below 70%. As shown in Fig. 6a, $Al(OH)_3$ and $NaAlF_4$ transformed into $Al(OH)_4^-$ at higher pH levels [26], leading to the dissolution of fluoride in the treated desorption solution. Therefore, a F/Al molar ratio of 1.0 was not suitable for the precipitation of Na_3AlF_6.

As shown in Fig. 9, HF was added into the desorption solution to adjust the initial F/Al molar ratio. The residual fluoride concentration decreased with increasing F/Al molar ratio. According to Fig. 7, the majority of aluminum

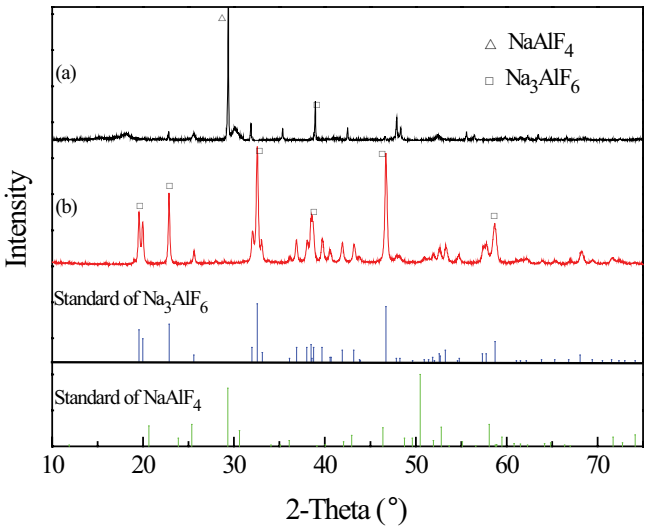

Fig. 10. XRD spectra of the recovered precipitations: (a) F/Al = 1, pH = 6.0 and (b) F/Al = 6, pH = 6.0.

was precipitated in the form of $Al(OH)_3$ at low F/Al molar ratios. Fluoride was not precipitated completely in the form of Na_3AlF_6, and the residual fluoride was kept in a solution with a high concentration. With the increased F/Al molar ratio, Na_3AlF_6 became the predominant solid phase. Na_3AlF_6 was more stable than $NaAlF_4$ with relatively low solubility. Therefore, the concentration of fluoride decreased at a high F/Al molar ratio.

The residual fluoride concentration of treated desorption solution decreased to 482.5–401.8 mg/L at a F/Al molar ratio of 5.0–6.0 and pH of 6.0. At this molar ratio, the recovery of fluoride was above 80%, and the comprehensive recovery of fluoride was above 90%. This demonstrated that the addition of HF decreased the residual fluoride concentration, and increased the recovery of fluoride. As shown in Fig. 10b, the phase of the precipitate matched the standard phase of Na_3AlF_6. Furthermore, the results of the batch experiment were consistent with the thermodynamic model. Therefore, the fluoride in the desorption solution could be recovered as Na_3AlF_6 when the reaction pH and the F/Al molar ratio were controlled.

4. Conclusions

To determine the feasibility of desorbing and recovering fluoride from an Al-loaded D751 resin, the desorption abilities of the fluoride-carrying resin and treatments for the desorption solution were investigated. The main results were:

NaOH was a more suitable desorption reagent than HCl. The fluoride desorption ratio surpassed 80% after 30 min when the NaOH concentration was 2.0–10.0 mol/L, and the liquid/solid ratio of V_d to m_a was 4:1–10:1. The fluoride concentration of the desorption solution was 2.8–12.8 g/L when the F/Al molar ratio was 0.96–1.00. The F/Al molar ratio and reaction pH were the main factors determining the recovery of fluoride from the desorption solution. More than 80% of the fluoride was recovered as cryolite

when a F/Al molar ratio of 5.0–6.0 and a pH of 6.0 was maintained by adding HF and HCl. The residual fluoride concentration of the desorption solution decreased from 3,508.2 mg/L to 401.8–482.5 mg/L. This provides a potentially effective way to desorb fluoride from cheating resins, and for the recovery of fluoride from desorption solutions as a valuable cryolite product.

Acknowledgments

This research was supported by the Natural Science Foundation of Hunan, China (2019JJ70016) and the Scientific Research Project of Hunan Education Ministry, China (18C1797).

References

[1] H. Huang, J. Liu, P. Zhang, D. Zhang, F. Gao, Investigation on the simultaneous removal of fluoride, ammonia nitrogen and phosphate from semiconductor wastewater using chemical precipitation, Chem. Eng. J., 307 (2017) 696–706.
[2] K. Jiang, K.G. Zhou, Removal and recovery of fluoride from wastewater by crystallization: effect of aluminum, Sep. Sci. Technol., 54 (2019) 1241–1246.
[3] B. Palahouane, N. Drouiche, S. Aoudj, K. Bensadok, Cost-effective electrocoagulation process for the remediation of fluoride from pretreated photovoltaic wastewater, J. Ind. Eng. Chem., 22 (2015) 127–131.
[4] J. Singh, P. Singh, A. Singh, Fluoride ions vs removal technologies: a study, Arab. J. Chem., 9 (2016) 815–824.
[5] J. Kim, B. Guillaume, J. Chung, Y. Hwang, Critical and precious materials consumption and requirement in wind energy system in the EU 27, Appl. Energy, 139 (2015) 327–334.
[6] N. Drouiche, N. Ghaffour, S. Aoudj, M. Hecini, T. Ouslimane, Fluoride removal from photovoltaic wastewater by aluminium electrocoagulation and characteristics of products, Chem. Eng. Trans., 17 (2009) 1651–1656.
[7] S. Aoudj, A. Khelifa, N. Drouiche, M. Hecini, Removal of fluoride and turbidity from semiconductor industry wastewater by combined coagulation and electroflotation, Desal. Water Treat., 57 (2016) 18398–18405.
[8] L. Deng, Y. Liu, T. Huang, T. Sun, Fluoride removal by induced crystallization using fluorapatite/calcite seed crystals, Chem. Eng. J., 287 (2016) 83–91.
[9] K. Jiang, K.G. Zhou, Recovery and removal of fluoride from fluorine industrial wastewater by crystallization process: a pilot study, Clean Technol. Environ. Policy, 19 (2017) 2335–2340.
[10] A.H. Wang, K.G. Zhou, X. Liu, F. Liu, Q. Chen, Development of Mg–Al–La tri-metal mixed oxide entrapped in alginate for removal of fluoride from wastewater, RSC Adv., 7 (2017) 31221–31229.
[11] S. Hamamoto, N. Kishimoto, Characteristics of fluoride adsorption onto aluminium(III) and iron(III) hydroxide flocs, Sep. Sci. Technol., 52 (2017) 42–50.
[12] G.C. Velazquez-Peña, M.T. Olguín-Gutiérrez, M.J. Solache-Ríos, C. Fall, Significance of FeZr-modified natural zeolite networks on fluoride removal, J. Fluorine Chem., 202 (2017) 41–53.
[13] Z. Bonyadi, P.S. Kumar, R. Foroutan, R. Kafaei, H. Arfaeinia, S. Farjadfard, B. Ramavandi, Ultrasonic-assisted synthesis of *Populus alba* activated carbon for water defluorination: application for real wastewater, Korean J. Chem. Eng., 36 (2019) 1595–1603.
[14] M.K. Uddin, S.S. Ahmed, M. Naushad, A mini update on fluoride adsorption from aqueous medium using clay materials, Desal. Water Treat., 145 (2019) 232–248.
[15] C. Castel, M. Schweizer, M.O. Simonnot, M. Sardin, Selective removal of fluoride ions by a two-way ion-exchange cyclic process, Chem. Eng. Sci., 55 (2000) 3341–3352.
[16] D.A.P. Tanaka, S. Kerketta, M.A.L. Tanco, T. Yokoyama, T.M. Suzuki, Adsorption of fluoride ion on the zirconium(IV) complexes of the chelating resins functionalized with amine-N-acetate ligands, Sep. Sci. Technol., 37 (2002) 877–894.
[17] F. Luo, K. Inoue, The removal of fluoride ion by using metal (III)-loaded amberlite resins, Solvent Extr. Ion Exch., 22 (2004) 305–322.
[18] N. Viswanathan, S. Meenakshi, Role of metal ion incorporation in ion exchange resin on the selectivity of fluoride, J. Hazard. Mater., 162 (2009) 920–930.
[19] C.S. Sundaram, S. Meenakshi, Fluoride sorption using organic–inorganic hybrid type ion exchangers, J. Colloid Interface Sci., 333 (2009) 58–62.
[20] G.J. Millar, S.J. Couperthwaite, D.B. Wellner, D.C. Macfarlane, S.A. Dalzell, Removal of fluoride ions from solution by chelating resin with imino-diacetate functionality, J. Water Process Eng., 20 (2017) 113–122.
[21] Y. Ku, H.M. Chiou, H.W. Chen, Removal of fluoride from aqueous solution by aluminum-loaded Duolite C-467 resin, J. Chin. Inst. Eng., 34 (2011) 801–807.
[22] S.M. Prabhu, S. Meenakshi, Effect of metal ions loaded onto iminodiacetic acid functionalized cation exchange resin for selective fluoride removal, Desal. Water Treat., 52 (2014) 2527–2536.
[23] G. Demirkalp, S. Alamut, Ö. Arar, Ü. Yüksel, M. Yüksel, Removal of Fluoride from water by Al(III)-loaded and $Al(OH)_3$-coated chelating resin, Desal. Water Treat., 57 (2016) 15910–15919.
[24] H. Paudyal, B. Pangeni, K. Inoue, H. Kawakita, K. Ohto, S. Alam, Removal of fluoride from aqueous solution by using porous resins containing hydrated oxide of cerium(IV) and zirconium(IV), J. Chem. Eng. Jpn., 45 (2012) 331–336.
[25] H. Paudyal, K. Inoue, H. Kawakita, K. Ohto, H. Kamata, S. Alam, Removal of fluoride by effectively using spent cation exchange resin, J. Mater. Cycles Waste Manage., 20 (2018) 975–984.
[26] K. Jiang, X. Pan, H. Zhou, Static adsorption of fluoride in aqueous solution by the D751 resin, Chem. Res. Appl., 32 (2020) 2061–2066.
[27] K. Jiang, K.G. Zhou, Y.C. Yang, H. Du, A pilot-scale study of cryolite precipitation from high fluoride-containing wastewater in a reaction-separation integrated reactor, J. Environ. Sci., 25 (2013) 1331–1337.
[28] M.A. Ford, J.d.B. Cunliff, An equilibrium model for the precipitation of synthetic cryolite, Hydrometallurgy, 16 (1986) 283–299.
[29] K.M. Steel, J. Besida, T.A. O'Donnell, D.G. Wood, Production of ultra clean coal part II—ionic equilibria in solution when mineral matter from black coal is treated with aqueous hydrofluoric acid, Fuel Process. Technol., 70 (2001) 193–219.
[30] S. George, P. Pandit, A.B. Gupta, Residual aluminium in water defluoridated using activated alumina adsorption–modeling and simulation studies, Water Res., 44 (2010) 3055–3064.
[31] D.F. Lisbona, K.M. Steel, Recovery of fluoride values from spent pot-lining: precipitation of an aluminum hydroxyfluoride hydrate product, Sep. Purif. Technol., 61 (2008) 182–192.
[32] C.Y. Tai, P.C. Chen, T.M. Tsao, Growth kinetics of CaF_2 in a pH-stat fluidized-bed crystallizer, J. Cryst. Growth, 290 (2006) 576–584.

Supporting information

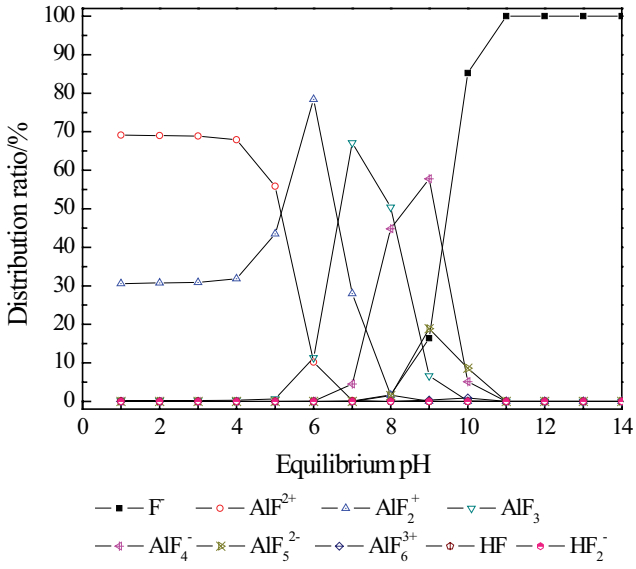

Fig. S1. Distribution ratio of the fluoride species (F/Al molar ratio = 1.0).

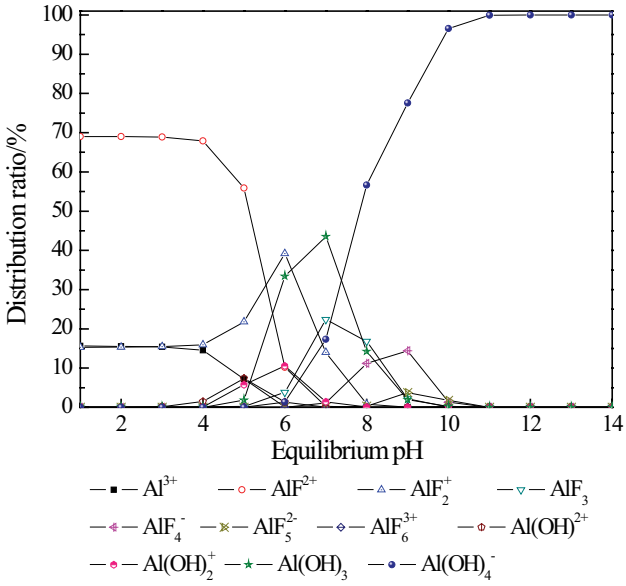

Fig. S2. Distribution ratio of the aluminum species (F/Al molar ratio = 1.0).